Modelling the occurrence of bouncing in droplet collision for different liquids

Maohong Sui*, Martin Sommerfeld[1], Lars Pasternak[1]
[1]Otto-von-Guericke-University Magdeburg, Multiphase Flow Systems, Institute for Process Engineering, Zeppelinstraße 1, D-06130 Halle (Saale), Germany
*Corresponding author: maohong.sui@ovgu.com

Abstract
Spraying systems are of great importance in a range of different technical and industrial applications. Depending on the operational conditions and the spray structure the produced droplet size spectrum may be largely affected by collisions between droplets. For the purpose of a numerical prediction of spraying processes by the Euler/Lagrangian approach, reliable models are required for predicting the collision outcome. This is mainly done by using so-called collision maps to demark the different outcome scenarios by appropriate boundary lines (i.e. bouncing, separation and coalescence). These boundary lines should be reasonably general including all relevant influential effects, such as impact conditions, droplet size ratio and liquid properties. Therefore, a variety of detailed experimental studies on the collision of higher viscous pure liquids and solution droplets were used for developing a model for the boundary line between coalescence and stretching separation. However, the boundary line for bouncing, mostly used in numerical studies so far was derived based on experiments with ethanol droplets [1]. And it completely neglects viscous dissipation. Therefore, the deviations for predicting the region of bouncing are quiet large for liquids with high viscosity or different properties. In this work, a new, more general correlation for the bouncing boundary is derived, which however includes new assumptions and definitions. The new boundary line is based on the studies of Estrade et al. [1] and Hu et al [2]. The original model has already been included a shape parameter ϕ' that actually also should be dependent of the impact parameter B which reflects the deformation during the collision process. Moreover, an additional parameter β has included to reflect the degrees of dissipation or the energy conversion during collision. Both parameters could be linearly correlated with the impact parameter B. The involved slope and initial values could be very well correlated with the Ohnesorge number and approximated by third order polynomials which fitted the available experimental results. However, the slopes and initial values are different for pure fluids and solution droplets. The new bouncing boundary line has been developed based on experimental result by Kuschel and Sommerfeld [3][4], Pasternak and Sommerfeld [5] [6]. Consequently, the boundary line for bouncing is predicted more accurately and the trends with changing liquid properties is very well captured.

Keywords
Droplet collision, collision map, bouncing boundary, viscosity effects, energy dissipation

Introduction

In order to model the outcome of droplet collisions with Euler/Lagrangian methods applied to sprays, the well-known collision maps are used. In this diagram the collision Weber-number(see appendix for definition) is plotted versus the non-dimensional impact parameter B (lateral droplet displacement upon collision), see Fig. 1, which shows the outcome of droplets collisions. Those outcomes are bouncing, coalescence, stretching as well as reflexive separation. However, these collision maps are not universally applicable. The outcomes depend on numerous parameters, such as liquid properties and droplet size ratio as well as surrounded fluid properties.

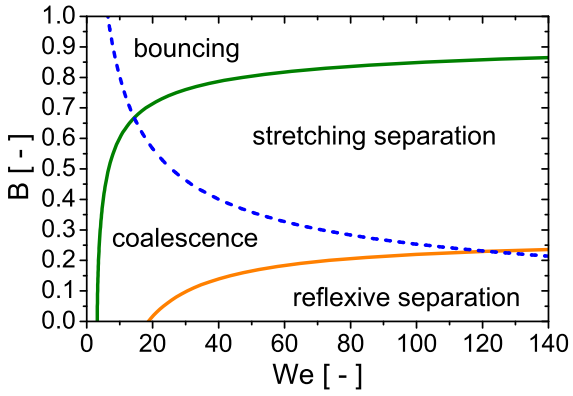

Figure 1. Typical droplet collision map including boundary lines between collision outcomes.

In order to get more accurate calculation results with the Euler/Lagrangian method, the boundary lines are essential to be properly correlated with liquid properties and other parameters. Most of them were obtained using an energy balance for the relevant collision scenario. The boundary between coalescence and reflexive separation may be properly fitted with the model of Ashgriz and Poo [7] for water droplets, but it is not suitable for liquids with higher viscosity [8]. The boundary between stretching separation and coalescence is quite often described by using the models of Brazier-Smith et al [9] and Ashgriz and Poo [7]. Both models do not take account for dissipation during the collision, droplets deformation and separation process. Only the momentum balance model of Jiang et al [10] accounts for energy dissipation and hence viscosity effects are included. This model was found to be adaptable for a range of viscosities when properly adjusting the two included model parameters by Gotaas et al [8]. The experiments were conducted for glycols with dynamic viscosities between 20 and 50 mPa·s. Similar findings were presented by Kuschel and Sommerfeld [3] for different solution droplets where the rise of solids content yields growing dynamic viscosity. Thereby, also an upward shift of the boundary line between stretching separation and coalescence was found, which could be characterized by a characteristic movement of the triple point. A generalized modelling of boundary lines between the different collision scenarios was first attempted in a follow-up research paper [3] by using a structure parameter describing transition phenomena in fluid flows. The lower boundary for bouncing was derived by Estrade et al. [1] based on experimental studies with Ethanol droplets. However, similar with the boundary generated by Ashgriz and Poo [7], this boundary line has not included the viscosity dissipation. In this paper, The new bouncing boundary line has been developed based on experimental result by Kuschel and Sommerfeld [3] [4] Pasternak and Sommerfeld [5].

Results and discussion

The new boundary line for bouncing is based on Estrade et al.[1] and Hu et al. [2]. Then, in order to include viscous dissipation, a new parameter called conversion rate β is introduced, with consideration of viscous dissipation.

$$KE_{in} + SE_{in} = SE_{md} + KE_{md} + VDE \tag{1}$$

$$KE_{in} = \frac{1}{2}\rho_l \pi \left(\frac{d_s^3 u_s^2 cos^2\theta}{6} + \frac{d_l^3 u_l^2 cos^2\theta}{6} \right) \tag{2}$$

$$u_s = \frac{u_r}{(1+\Delta)^3} \quad u_l = \frac{u_r \Delta^3}{(1+\Delta)^3} \tag{3}$$

Eq.(3) considers the entire droplet volume, instead of the interaction region of colliding droplets in the model of Estrade [1].

$$KE_{in} = \frac{d_l^2 \pi \Delta^2 (1-B^2)}{12(1+\Delta^3)} \rho_l u_r^2 d_s \tag{4}$$

From the definition of surface tension energy, the surface energy can be expressed as below.

$$SE_{in} = \sigma\pi(d_s^2 + d_l^2) = \sigma\pi d_l^2 (1+\Delta^2) \tag{5}$$

The conversion rate β is defined as the percentage of energy that does not convert to surface energy at maximum deformation during droplets collision.

$$KE_{in} + SE_{in} = SE_{md} + (KE_{md} + VDE) = SE_{md} + \beta KE_{in} \tag{6}$$

From experimental observation, all the initial kinetic energy is converted to surface energy and viscous dissipation energy (KE_{md}=0) at the moment of maximum deformation when it is head-on collision (at B=0), due to the deformation of droplets. However, with impact parameter B increasing, the deformation of droplets would become smaller. Then the viscos dissipation and the surface energy at maximum deformation would also be less. On contrast, when the impact parameter is less than 0.3, the remaining kinetic energy would be larger, which would explain the trajectory of droplets, the upper limit of reflexive separation boundary line from Ashgriz et al. [7], the collided droplets would bounce away and make reflection. While the impact parameter is larger than 0.3, for bouncing, the droplets would generally continue their trajectories. The effect of the rotational motion of droplets could be neglected.
As shown in Fig. 2 [1], bouncing occurs when $h_s \leqslant \phi r_s$ and $h_l \leqslant \phi r_l$, where ϕ is defined as the ratio h_s/r_s or h_l/r_l beyond where coalescence or separation occurs. These conditions and the mass conservation of the two droplets permit the following relations to be written: $h_l \leqslant d_l^3 \sqrt{1+\frac{3}{\phi^2}}$ and $h_s \leqslant d_s^3 \sqrt{1+\frac{3}{\phi^2}}$.
Then it results:

$$Es_{md} \geqslant \frac{1}{3}\sigma\pi d_l^2 (1+\Delta^2)(2(\frac{3}{\phi^2}+1)^{-\frac{2}{3}} + (\frac{3}{\phi^2}+1)^{\frac{1}{3}}) \tag{7}$$

$$\phi' = 2(\frac{3}{\phi^2}+1)^{-\frac{2}{3}} + (\frac{3}{\phi^2}+1)^{\frac{1}{3}} \tag{8}$$

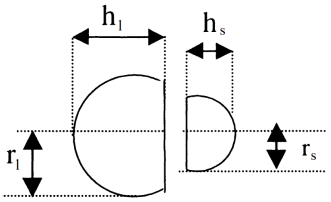

Figure 2. Model of droplet deformation when bouncing according to experimental observations.[1]

$$We = \frac{(1+\Delta^2)(1+\Delta^3)(-12+4\phi')}{(1-B^2)(1-\beta)\Delta^2} \tag{9}$$

After the observation of the results from experiments, it is obvious that the shape parameter ϕ' is not constant for droplet collisions with different impact parameter B. Not only the relative velocity, but also the liquid properties would have effect on it, for example, liquids with larger viscosity are harder to deform. And according to the definition of ϕ and ϕ', the range of them should be larger than 2 and smaller than 3, respectively.
For β, it contains 2 parts, one is the kinetic energy remaining in the droplets, another is the viscous dissipation energy. In experimental research of Jiang et al. [10], for the lower limit of B(B=0) and at maximum deformation condition, it is discovered that about 50% of the total energy is lost, due to viscous dissipation. And at the mean time the relative velocity is 0, which means there is no remaining kinetic energy in the droplets. Consequently, the conversion rate ($\beta = 0.5$) for droplets at head-on collision $B = 0$ can be accepted. Furthermore, the upper limit of impact parameter B=1, there is no kinetic energy converted to surface energy, then the conversion rate $\beta = 1$. Moreover, parameter β would also be influenced by liquid properties. Thus, Ohnesorge number(Oh) is introduced as a relevant parameter.

Assumption
For both ϕ' and β, it is assumed that they are linearly related with the impact parameter B. The shape parameter ϕ' decreases down to the lower limit 3 according to the definition of shape factor. And β increases to the upper limit 0.5. This results,

$$\phi'(B) = -k_{\phi'}(Oh) * B + \phi'_{initial}(Oh) \tag{10}$$

$$\beta(B) = k_{\beta}(Oh) * B + \beta_{initial}(Oh) \tag{11}$$

The initial shape parameter $\phi'_{initial}$ and conversion rate $\beta_{initial}$ are interceptions of their profile versus Oh, which represents the moment of maximum deformation. According to the results of pure liquid and solutions [3][4] , the correlations are generated. As shown in Fig. 3, from the correlation of ϕ' and β, it is obvious that the shape parameter ϕ' performs differently in pure liquids and solutions. But the conversion rate β is not. The data for both liquids follow the same trend.

$$\begin{cases} k_{\phi',pureliquid} = -30.98Oh^3 + 20.40Oh^2 - 4.95Oh + 0.77 \\ \phi'_{initial,pureliquid} = -33.41Oh^3 + 23.18Oh^2 - 5.81Oh + 3.9 \end{cases} \tag{12}$$

$$\begin{cases} k_{\phi',solution} = -2.8Oh^3 + 3.59Oh^2 - 1.35Oh + 0.21 \\ \phi'_{initial,solution} = 14.3Oh^3 - 5.43Oh^2 - 0.39Oh + 3.31 \end{cases} \tag{13}$$

$$\beta_{initial} = \begin{cases} 23.97Oh^3 - 19.50Oh^2 + 5.07Oh + 0.08 & Oh \leqslant 0.15 \\ \beta_{initial} = 0.5 & Oh > 0.15 \end{cases} \tag{14}$$

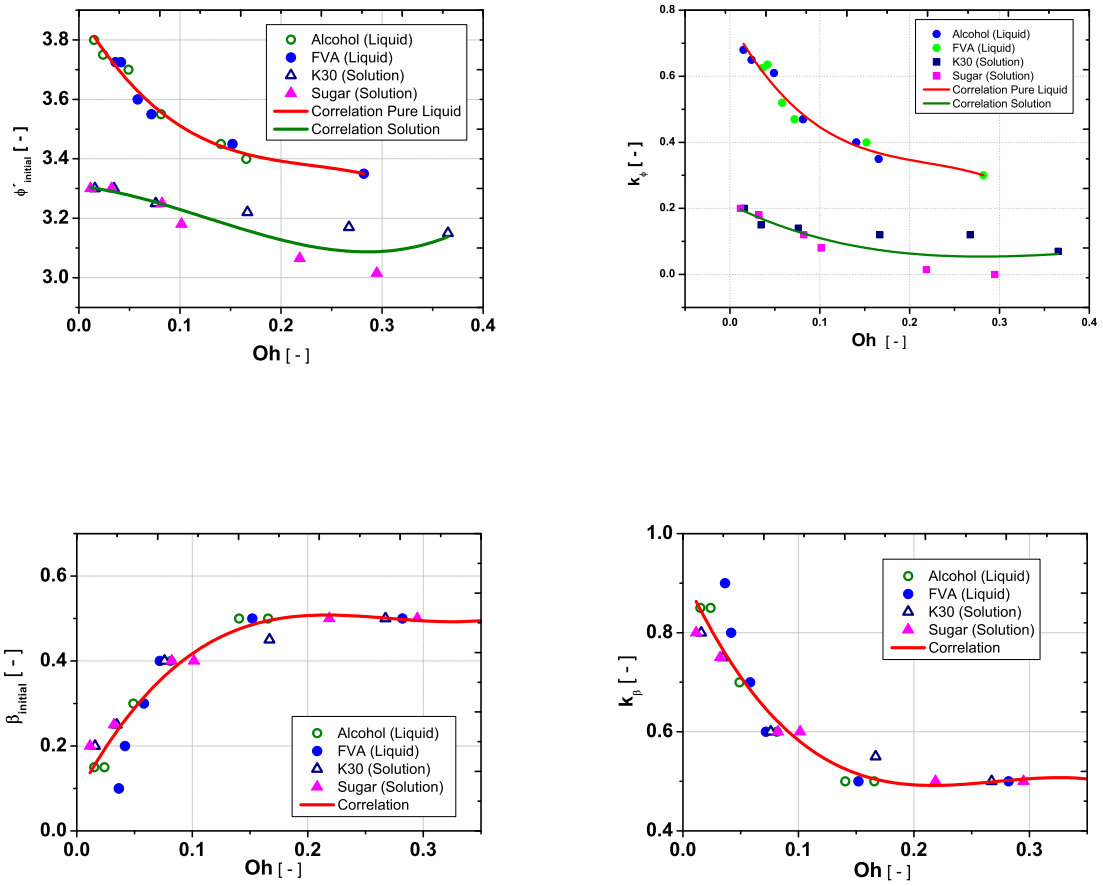

Figure 3. The values of the shape parameter ϕ' and the conversion rate β extracted from the experiment with suggested polynomials

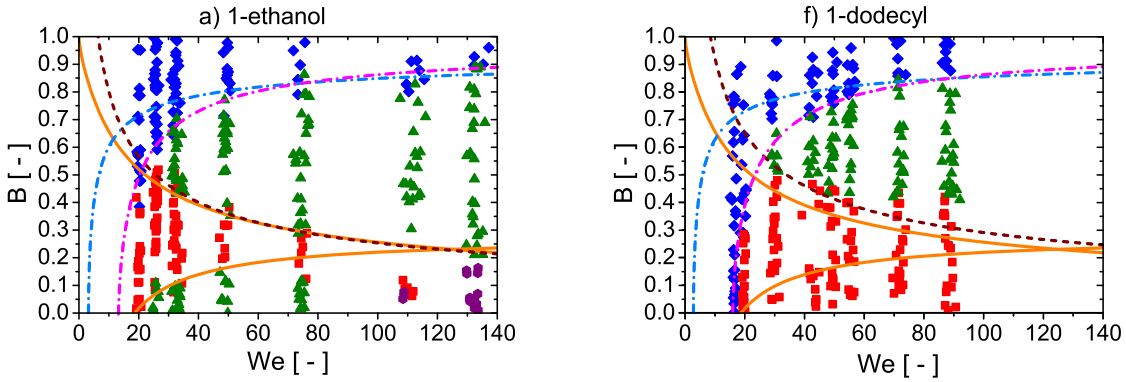

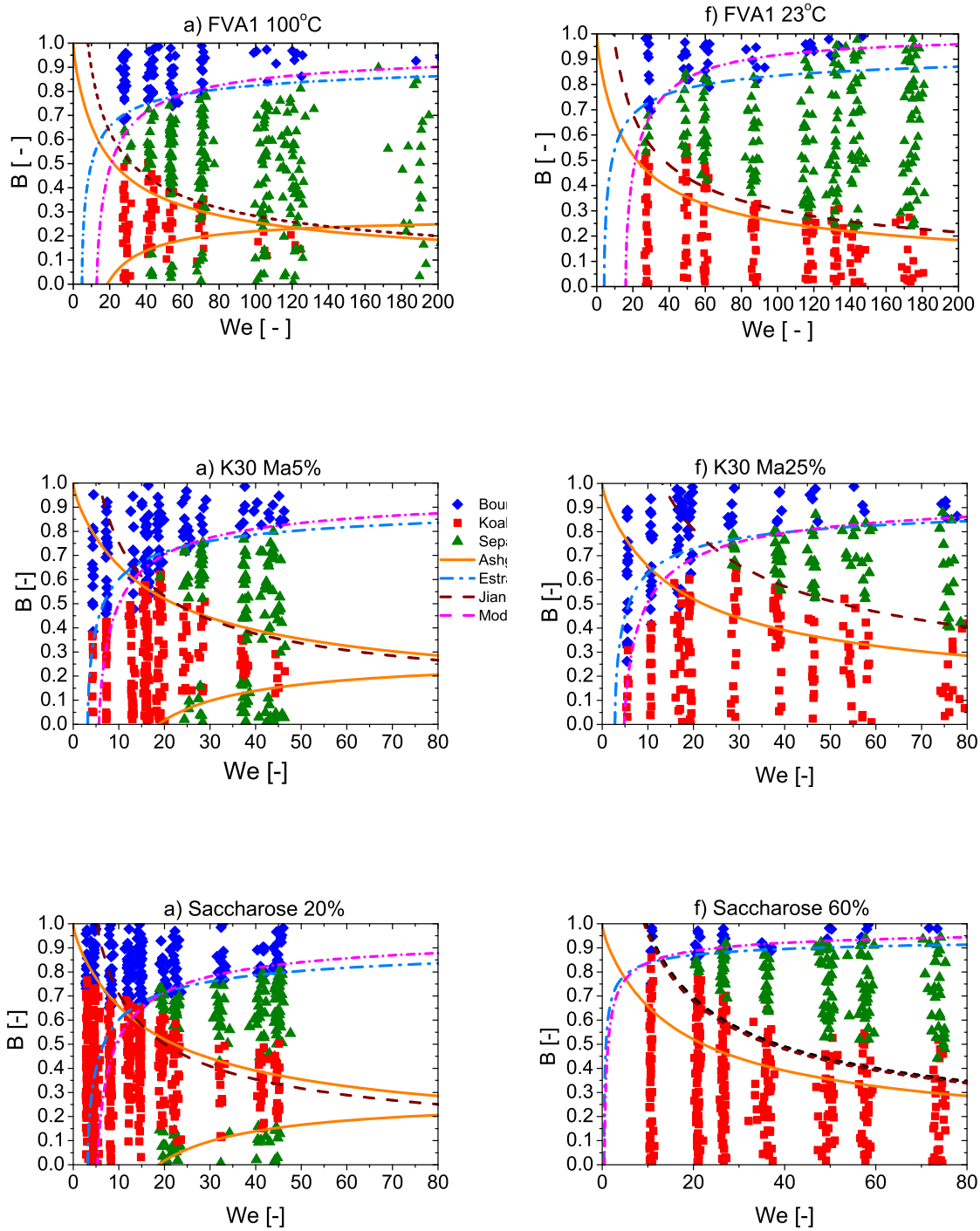

Figure 4. Measured collision outcome in the B-We diagram for different liquids[4][3].
(Blue Dashed dotted line model of Estrade[1], Magenta continuous line model of new equation.)

Collision Maps

With respected to the collision maps, there are 4 groups of experimental data considered with, portion of which are shown in Fig. 4. All these data come from Sommerfeld and Kuschel [3] [4]. Group A,B,C,D are pure liquid of alcohols, the pure liquid of FVA in different temperature, polyvinylpyrrolindone solution PVP K30 5-25Ma% solution and Saccharose 20-60Ma% solution respectively. All these liquids covers a range of dynamic viscosity from 1 to 60 $mPa \cdot s$. The experiments were conducted under air pressure 1 bar. Detailed properties are summarized in Table. 1.

The new bouncing boundary shows much better corresponding compared with the previous study [1]. While in lower bouncing region (We<30), it shows more curvature considering viscous dissipation; in higher bouncing region (We>60), the viscosity dissipation is minor, which also fit the experiment results better. It should be noted, all the experiments data in this paper only consider a size ratio of $\Delta = 1$. Further research would be continued on the effect of different size ratio.

Conclusions

A predictive model is suggested for the determination of the boundary line for bouncing in droplet collisions. This model is based on the energy balance approach with the idea of included a term for viscous dissipation energy. The involved model parameters are adapted according to experimental observations using correlations with the Ohnesorge number, which depends on the liquid properties and droplet size only.

Acknowledgements

The author acknowledges the financial support of this research project by the China Scholarship Council (CSC) under contract Nr. 201708080130. Furthermore, thanks to the guidance from Prof. Martin Sommerfeld.

Nomenclature

KE_{in}	Initial kinetic energy	KE_{md}	Kinetic energy at maximum deformations
SE_{md}	Surface energy at maximum deformation	SE_{in}	Initial surface energy
VDE	Viscosity dissipation energy	ρ_l	Fluid density [kg/m^3]
d_s, d_l	Droplet diameters, small, large [m]	ϕ	The ratio h_s/r_s or h_l/r_l
u_{rel}	Relative velocity upon collision [m/s]	β	Converted rate
u_s, u_l	Droplet velocity, small, large [m/s]	ϕ'	The shape parameter
μ	Dynamic viscosity [mPa·s]	σ	Surface tension [N/m]
θ	Droplet collision angle °		

Appendix

The definitions of the relevant non-dimensional parameters to describe binary collisions of liquid droplets with identical viscosity as well as to create the collision maps are given below:

Reynolds number Re: $$Re = \frac{\rho d_s u_{rel}}{\mu}$$

Collision Weber number We: $$We = \frac{\rho d_s u_{rel}^2}{\sigma}$$

Impact parameter B: $$B = \frac{2b}{d_s + d_l} = sin\theta$$

Capillary number Ca: $$Ca = \frac{\mu}{\sigma} u_{rel} = \frac{u_{rel}}{u_{relax}}$$

Ohnesorge number Oh: $$Oh = \frac{\mu}{\sqrt{\rho \sigma d_s}}$$

Droplet size ratio Δ: $$\Delta = \frac{d_s}{d_l}$$

Table 1. The parameters of experiment liquids

	Oh	$\phi'_{initial}$	$k_{\phi'}$	$\beta_{initial}$	k_β
Ethanol	0.0150	3.8	0.68	0.15	0.9
Propanol	0.0240	3.75	0.65	0.15	0.9
Hexanol	0.0490	3.7	0.61	0.3	0.7
Heptanol	0.0813	3.55	0.47	0.4	0.6
Nonanol	0.1405	3.45	0.4	0.5	0.5
Dodecanol	0.1656	3.4	0.35	0.5	0.5
FVA1 100℃	0.0364	3.725	0.63	0.1	0.9
FVA1 90 ℃	0.0417	3.725	0.64	0.2	0.8
FVA1 70 ℃	0.0581	3.6	0.52	0.3	0.7
FVA1 60℃	0.0718	3.55	0.47	0.4	0.6
FVA1 45 ℃	0.1520	3.45	0.4	0.5	0.5
FVA1 23℃	0.2820	3.35	0.3	0.5	0.5
PVP K30 Ma5%	0.0158	3.3	0.2	0.2	0.8
PVP K30 Ma10%	0.0347	3.3	0.15	0.25	0.8
PVP K30 Ma15%	0.0760	3.25	0.14	0.4	0.6
PVP K30 Ma20%	0.1668	3.22	0.12	0.45	0.6
PVP K30 Ma23%	0.2673	3.17	0.12	0.5	0.5
PVP K30 Ma25%	0.3653	3.15	0.07	0.5	0.5
Saaccharose Ma20%	0.0115	3.3	0.2	0.2	0.8
Saaccharose Ma40%	0.0323	3.3	0.18	0.25	0.8
Saaccharose Ma50%	0.0822	3.25	0.12	0.4	0.6
Saaccharose Ma54%	0.1015	3.18	0.08	0.4	0.6
Saaccharose Ma58%	0.2186	3.06	0.02	0.5	0.5
Saaccharose Ma60%	0.2949	3.015	0	0.5	0.5

References

[1] Estrade, J. P., et al., 1999. *International Journal of Heat and Fluid Flow,* **20**(5), Oct., pp. 486–491.
[2] Hu, C., et al., 2017. *International Journal of Heat and Mass Transfer,* **113**, Oct., pp. 569–588.
[3] Kuschel, M., and Sommerfeld, M., 2013. *Experiments in Fluids,* **54**(2), Feb.
[4] Sommerfeld, M., and Kuschel, M., 2016. *Experiments in Fluids,* **57**(12), Dec.
[5] Pasternak, L., and Sommerfeld, M., 2017. In Ilass Europe. 28th european conference on Liquid Atomization and Spray Systems, Editorial Universitat Politècnica de València, pp. 710–715.
[6] Sommerfeld, M., and Pasternak, L., 2019. *International Journal of Multiphase Flow,* **117**, Aug., pp. 182–205.
[7] Ashgriz, N., and Poo, J. Y., 1990. *Journal of Fluid Mechanics,* **221**, Dec., pp. 183–204.
[8] Gotaas, et al., 2007. *Physics of Fluids,* **19**(10), Oct., p. 102106.
[9] Brazier-Smith, P. R., et al., 1972. *Proc. R. Soc. Lond. A,* **326**(1566), Jan., pp. 393–408.
[10] Jiang, Y. J., et al., 1992. *Journal of Fluid Mechanics,* **234**, Jan., pp. 171–190.